A Numerical Study on the Effect of Initial Void Ratio and Areal Extent of Heterogeneity on Instability Onset in Granular Media

Debayan Bhattacharya and Amit Prashant

Abstract The present study numerically explores the coupled biaxial undrained instability analysis of Hostun RF sand with varying initial void ratio (e_0) for a given confining pressure (σ'_c). A transient analysis of 100 mm × 100 mm sand specimen has been carried out with the implementation of a generalized 3D nonassociative elastoplastic material model. Finite element analysis has been performed in ABAQUS v6.14 and the constitutive model has been incorporated by scripting a user-defined material model subroutine (UMAT). The standard custom for instability analysis involves introduction of some form of heterogeneity within the material domain (perturbation) and probing its response against the prescribed boundary conditions. Mesh sensitivity of instability onset has been explored in the current context numerically while material imperfection has been introduced in terms of e_0. The coupled analysis allowed local fluid motion within the material continuum, while the undrained boundary condition was imposed globally. Instability onset gets delayed as e_0 is decreased (relatively denser specimens) for a given σ'_c with distinct signatures of dilative and contractive zones existing adjacent to each other (for specimens with e_0 < critical void ratio (e_c)) for a particular perturbation magnitude. Influence of spatial extent of heterogeneity for a given perturbation intensity and σ'_c also showed some effect in lowering down the instability onset strain to some degree and ceased to display significant impact on further increase in the areal extent of material imperfection.

Keywords Sand · Instability · Strain localization · Plane strain · Transient analysis · Perturbation

D. Bhattacharya · A. Prashant (✉)
Indian Institute of Technology Gandhinagar, Gandhinagar, India
e-mail: ap@iitgn.ac.in

D. Bhattacharya
e-mail: debayan.bhattacharya@iitgn.ac.in

A. Prashant et al. (eds.), *Advances in Computer Methods and Geomechanics*, Lecture Notes in Civil Engineering 55,
https://doi.org/10.1007/978-981-15-0886-8_28

1 Introduction

A soil specimen analysed in the laboratory is inherently heterogeneous in nature although the measurements are accomplished considering it as a single element. However, it is these inherent material imperfections that lead to the specimen exhibiting non-uniform deformation modes suddenly from a state of uniform homogeneous material response and leading to instability in granular materials. This state is coined as bifurcation of the material behaviour and the localized plastic strain accumulation associated with it is an omnipresent feature of granular media undergoing non-uniform deformations. Experimental findings report that plastic instabilities are often encountered in the form of localized zones of extensive shearing (deformation bands), bulging of the specimen or buckling of surfaces and volume instability [8–11, 17–20, 24]. The emergence of these plastic instabilities suddenly from the uniform stress–strain state depends on the material properties, type of loading, boundary and drainage conditions [27, 28]. These deformation bands essentially form the weak planes and are found to exist in various geologic materials (e.g. soil, rock, concrete, etc.) in the form of fault gouges, shear bands etc. [6]. In addition to this, fluid flow within the fully saturated porous media not only affects the strength of these materials, but also influences the movement of fluids entrapped (e.g. gases, hydrocarbons, etc.) within it [3]. Strain localization is one such ubiquitous feature in geomaterials and acts as a precursor to failure that may result in sudden collapse of earthen embankments, etc., particularly in an undrained situation (rapid drawdown case) by virtue of which, investigation regarding its onset is of main concern in contemporary geomechanics research.

The experimental findings and the theoretical predictions related to dense sand specimens exhibiting persistent shear bands under drained conditions (allowing global volume change) are in good agreement with each other and have been explored extensively in the past by several researchers [10, 11, 17]. On the contrary, instability studies related to soil specimens under (globally) undrained conditions reported contrasting account of observations [9, 11, 18, 19, 21, 22]. Nucleation of shear bands in conjugate arrays has been reported to initiate in sand specimens during initial stages of loading while performing an undrained test, which later manifests itself into a distinct zone of extensive strain accumulation. These localized zones are dilative in nature accompanied by contractive zones adjacent to them which reveal local fluid movement within the material continuum although global isochoric condition (constant volume—globally undrained) was imposed on the sand specimen [15, 16]. This signature exhibited by granular media gives the motivation to carry out a coupled undrained instability analysis in sands by incorporating transient diffusion process for the fluid flow in the present study.

Numerical investigation (FEM analysis) of the strain localization phenomenon in granular media has received much attention in past few decades in the form of several noteworthy contributions by Borja and Regueiro [7]; Fleck and Hutchinson [12]; Bažant and Jirásek [4] etc. owing to its various ‘pathological’ issues. A significant amount of effort has been devoted so as to model the strain-softening behaviour and

shear banding phenomenon acceptably well within the realms of continuum mechanics. Nevertheless, the onset of instability in pressure-dependent elastoplastic solids and the post-localization material response are two different features and should be dealt with separately. The present study deals with numerical investigation of instability onset in granular media by introducing some form of perturbation(weak element) in the material domain and checking its response against the prescribed boundary conditions. This calls for a standard mesh convergence study with material imperfection (for a particular perturbation intensity) and also aims at matching the theoretically predicted instability onset strain as reported by Mukherjee et al. [23] on Hostun RF sand. A theoretical study has been carried out by Mukherjee et al. [23] within the bifurcation analysis framework on Hostun RF sand with varying densities, confining pressure and boundary conditions—flexible as well as rigid to estimate the onset of instability in granular media. The emergence of two possible modes of instability in the form of localized zones of strain accumulation and 'liquefaction-type solid-fluid' instability has been reported in their study under rigid and flexible boundary conditions. The present study deals with undrained biaxial shearing of Hostun RF sand at a particular confining pressure and perturbation magnitude but with varying initial void ratio (e_0) so as to explore its effect on the instability onset strain.

2 Plane Strain Problem Formulation—Geometry and Material Model

Figure 1 illustrates the schematic representation of a biaxially loaded saturated sand specimen of 100 mm × 100 mm size. No shear stress has been considered in any of the boundaries. Plane strain biaxial shearing of the sand specimen (deformation rate = 0.1 mm/min) was accomplished under a globally undrained condition while

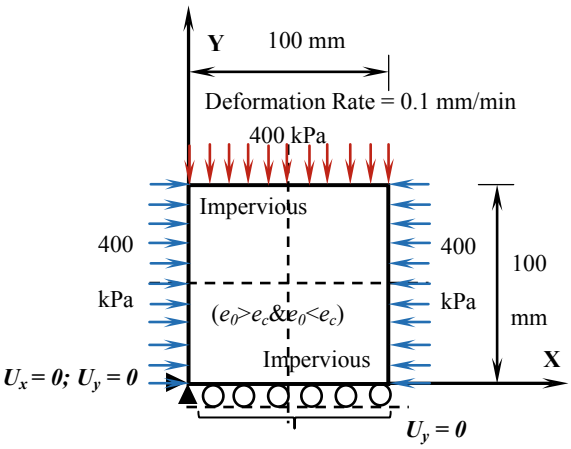

Fig. 1 Schematic illustration of biaxial plane strain problem showing geometry and boundary conditions

local fluid movement within the porous granular media was allowed. Both vertical and horizontal movement were constrained at the leftmost bottom corner node of the sand specimen while rest of the bottom nodes allowed horizontal movement (roller support) only. The top as well as the bottom surfaces portray rigid boundary conditions with equal deformation at all nodes and the lateral boundaries on the other hand are flexible in nature.

Numerical investigation has been performed on Hostun RF sand specimens with different e_0 varying from 0.6 (dense sand specimens, $e_0 < e_c$) to 0.8 (loose specimens, $e_0 > e_c$) at a confining pressure of 400 kPa. Coupled equilibrium equations for the soil skeleton along with the continuity equation for fluid (water) flow have been considered in the present context. In order to incorporate a generalized 3D nonassociative elastoplastic constitutive relationship [29], a user-defined material model subroutine (UMAT) has been implemented within the numerical framework of ABAQUS v6.14. The material model has been formulated in the realms of Critical State theory [25] and it incorporates both shear as well as volumetric hardening [13]. It considers the widely used Mohr–Coulomb failure criteria and assimilates the stiffness and strength dependence on state parameter (ψ) with critical state theory. A hyperbolic relationship dictates the evolution of plastic stiffness while the flow rule has been drawn upon similar lines of Cam-Clay model within bounding-surface plasticity framework. The elastic response is considered to be linear while the yield surface (f) and the plastic potential function (g) governing the inelastic material behaviour are defined as,

$$f(\sigma', \varepsilon_q^p, \varepsilon_v^p) = \sqrt{3J_2} + \eta_y \frac{I_1'}{3} = 0;\ g(\boldsymbol{\sigma'}) = \sqrt{3J_2} + M_c \frac{I_1'}{3} \ln \frac{3P_r'}{I_1'} = 0 \quad (1)$$

In Eq. (1), ε_q^p and ε_v^p represent the shear and the volumetric plastic strains, respectively; I_1' and J_2 denote first invariant of the stress tensor and second invariant of the deviatoric stress tensor, respectively. M_c is the slope of critical state line in shear stress and $-I_1'/3$ plane; P_r' is the intercept of g on $-I_1'/3$ axis and η_y is the shear stress ratio (i.e. ratio of deviatoric stress q and mean effective stress p'), which is a state variable of the material model. Evolution of η_y is governed by ε_q^p which itself is dependent on another state variable (ψ) that incorporates the effect of p' and density of the specimen. Material parameters considered for the constitutive model have been adopted from Gajo and Wood [13] and Wood [29].

The porous media has been modelled with the aid of an Eulerian mesh i.e. the finite element (FEM) mesh of the soil skeleton is affixed to the fluid mesh. In order to carry out the undrained (globally undrained, locally drained) transient analysis, continuum stress/displacement (*C*) 8-noded plane strain (*PE 8*) quadrilateral, biquadratic displacement, bilinear pore pressure (*P*) elements (*CPE8P*) [1] have been utilized in the present study. The backward Euler approximation approach has been adopted in the current context to integrate the coupled variational forms of the continuity equation ensuring fluid flow within the specimen and equilibrium equations of the porous medium. These coupled equations have been solved at the nodal points by

employing full Newton-Raphson iteration scheme with the implementation of an unsymmetrical solver.

3 Mesh Sensitivity and Perturbation Intensity Dependence of Instability Onset

In a related study, Bhattacharya et al. [5], examined the instability onset during undrained (locally drained, globally undrained) biaxial shearing of Hostun RF sand specimens for a particular perturbation magnitude and confining pressure and reported that instability onset within a numerical framework is a mesh dependent phenomenon. The global force (F) displacement (δ) response (specimens with σ'_c = 400 kPa and e_0 = 0.65) for a small heterogeneity (0.01% of e_0) induced in the middle element of the specimen was found to be uniform for less number of elements (N = 9 or 16). However, finer mesh discretization resulted in drop in the F-δ response for 225 elements with axial strain at instability onset (ε^b_{ao}) reducing down to 3.3%. Interestingly, with further refinement of mesh, ε^b_{ao} reduced down to 1.77% and 1.37% for 400 and 625, elements, respectively, although it still followed the same homogeneous material response (F-δ) curve before instability onset (drop in F-δ response). The present discussion limits itself to investigation of instability onset in granular media only and does not delve into the post-localization material response. In this post-instability region, several governing factors (e.g. length scale, deformation rate and characteristic time scale) play a pivotal role in the mechanical response of granular media [14]. Although, a small perturbation was introduced in the material domain, ε^b_{ao} became almost asymptotic (Fig. 2) to the theoretically predicted (ε_{th}) value reported by Mukherjee et al. [23] at a finer mesh only and this is achieved at the cost of significant amount of computing time since the time increment (Δt) is proportional to the square of the element size $(\Delta l)^2$ during a transient analysis. Despite the fact transient diffusion process involved in the coupled analysis introduces an inherent length scale in the numerical simulations, they are not adequate enough to examine the post-instability material response [2] of the sand specimens.

Perturbation (weak element) intensity (P) significantly influences ε^b_{ao} and in order to explore this effect, material heterogeneity has been induced in the middle element (in terms of e_0) of the sand specimens i.e. by locally weakening the element. All the simulations exploring this effect have been probed with 400 elements (with σ'_c = 400 kPa and e_0 = 0.65) which was sufficient enough for the current analysis under consideration. The computational time for carrying out a transient undrained biaxial shearing of Hostun RF sand with the aid of Intel ® Core-TM i7-processor (4 Cores); 3.6 GHz clock speed was estimated to be around 15 ~ 16 h for 400 elements which heightened to 19 ~ 20 h for 625 elements—thus finer mesh discretization was avoided. Previous studies by Borja and Regueiro [7], Shuttle and Smith [26] report introduction of perturbation in terms of reduction of the value of material model (nonassociative Drucker-Prager type) parameter by 1% or by reducing the undrained

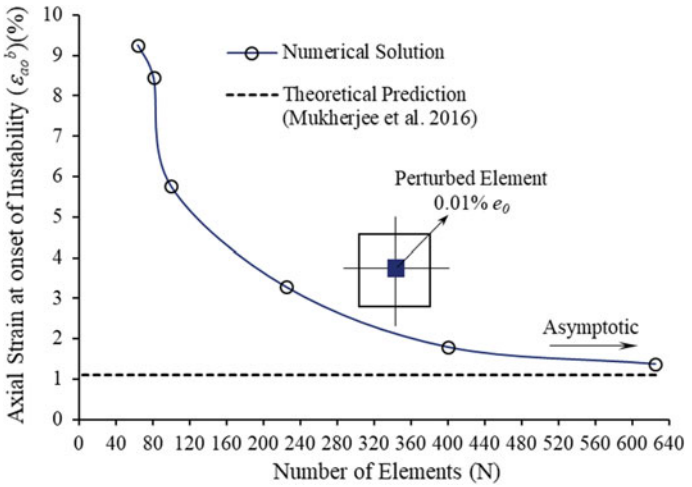

Fig. 2 Axial Strain at onset of instability (ε^b_{ao}) (%) versus number of elements (N) with perturbation intensity 0.01% e_0 (0.65) at middle element

cohesion (c_u) value to 20 kPa in the 'trigger element' as compared to 70 kPa for other elements throughout the specimen—but these were chosen intuitively and lacked a systematic study of perturbation intensity effect on instability onset strain. For $P =$ 0.1% and 2.5% ε^b_{ao} was estimated to be $\approx$ 1.78% and 1.6%, respectively (Fig. 3). Increased value of P to 10% of e_0 resulted in decrease of ε^b_{ao} to nearly ε_{th}. However, with $P = 25\%$ and 50% (very weak zone encountered within the soil mass), ε^b_{ao} was

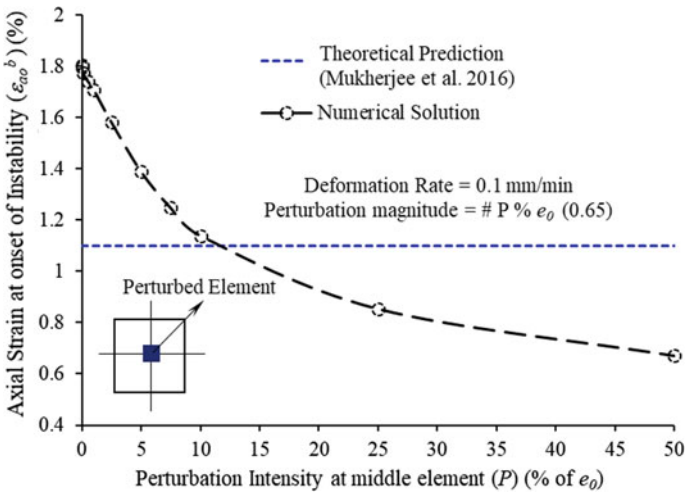

Fig. 3 Axial strain at onset of instability (ε^b_{ao}) (%) versus perturbation intensity (P # %of $e_0 =$ 0.65)

found to be well below ε_{th}. This points out a reasonable estimate of what should be the perturbation intensity so as to explore instability onset within any numerical framework.

Imperfection has been introduced within the material domain in terms of initial void ratio (e_0) in the current context in all the simulations, although it is acknowledged that the perturbation intensity effect may be somewhat different if the material heterogeneity is incorporated in terms of a state variable of the constitutive model and characterization of instability becomes material model-dependent phenomenon in that case.

4 Effect of Initial Void Ratio (e_0) on Instability Onset

The material state of the soil specimen (e.g. void ratio) is one of the key factors that can trigger instability (either localization or 'solid-fluid' type instability) onset in granular materials. The present study aims to examine this effect of the initial void ratio (e_0) on instability onset strain as well. For this purpose, undrained biaxial shearing has been carried out on all the sand specimens (e_0 varying from 0.6 to 0.8) at a confining pressure of 400 kPa with a perturbation intensity $P = 1\%$ of e_0 at the middle element. Figure 4a illustrates the F-δ response of various sand specimens with varying initial void ratios. For a dense specimen, with $e_0 = 0.6$ ($e_0 < e_c$), the drop in F-δ response i.e. instability onset was observed to be at $\varepsilon_{ao}^b \sim 4.75\%$ although the specimen exhibited strain hardening behaviour till this point of loading. On increasinge_0 to 0.65 ($e_0 < e_c$) (medium dense specimen), the sand sample still displayed a strain hardening behaviour although ε_{ao}^b reduced down significantly to ~ 1.71% and localized dilative zones were noticed along with contractive zones adjacent to it at this stage. For $e_0 = 0.7$ and 0.75 ($e_0 < e_c$, in both the cases), ε_{ao}^b was estimated to be ~ 0.9% and 0.74%, respectively. It can be noticed from Fig. 4a that the Hostun RF sand specimen with $e_0 = 0.75$ did not exhibit any strain hardening behaviour and this value of e_0 was very close to the critical void ratio (at $\sigma'_c = 400$ kPa), $e_c = 0.789$. When e_0 was further increased to 0.8 (loose specimen, $e_0 > e_c$), instability onset was estimated to occur at a much lower axial strain level ~ 0.5%. No drop in F-δresponse was observed in this case and the specimen was devoid of any distinct localized zones of extensive shearing. Strain softening behaviour could be noticed from F-δ plot for this sand specimen and the theoretical study byMukherjee et al. [23] also suggested that undrained strain softening behaviour is associated with 'liquefaction-type solid-fluid' instability modes in granular media. Thus, in this case, 'solid-fluid' type instability could have been triggered due to high initial void ratio (loose sand specimens) and generation of significant amount of excess pore water pressure during undrained shearing(locally drained, globally undrained). Figure 4b represents the variation in axial strain at instability onset, ε_{ao}^b with e_0. Lower initial void ratio of Hostun RF sand specimens (dense specimens) resulted in delayed (at the same confining pressure) onset of instability indicating a decisive

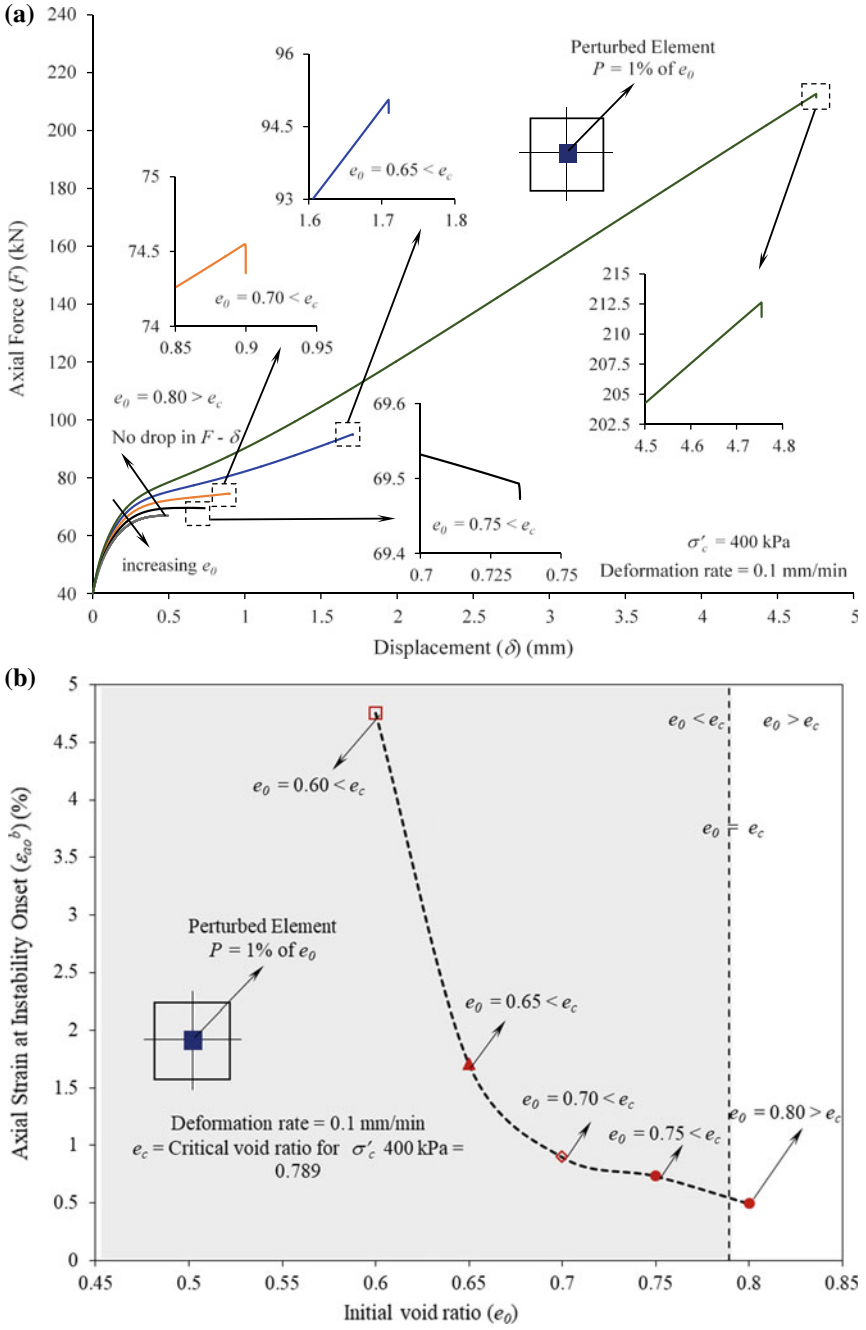

Fig. 4 **a** Force (F)—displacement (δ) plot for Hostun RF sand specimens with varying initial void ratio (e_0) (0.6–0.8). **b** Axial strain at onset of instability (ε_{ao}^{b}) (%) versus e_0

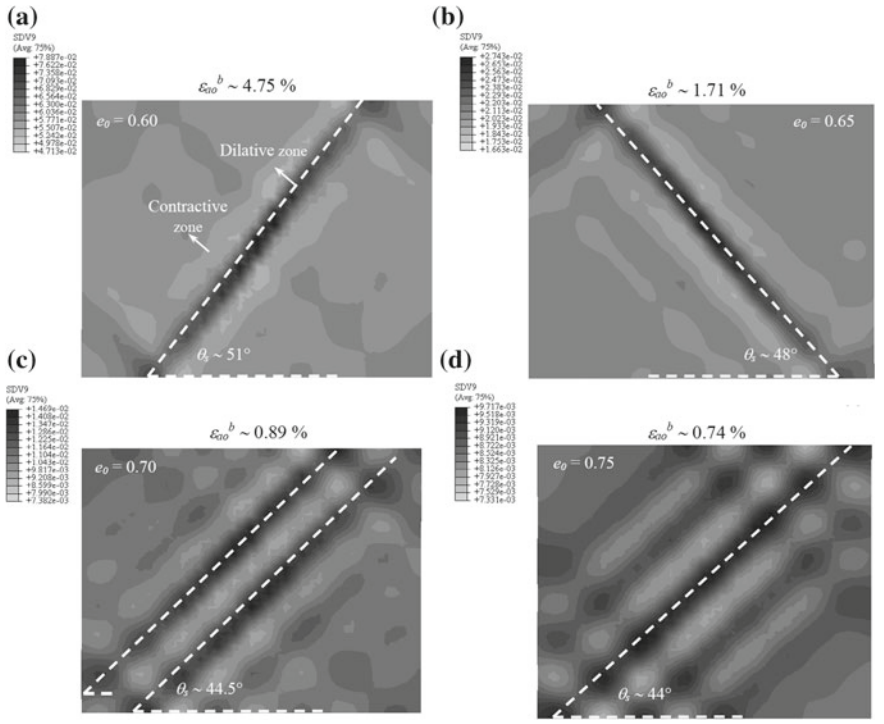

Fig. 5 Shear strain (SDV9) (ε_q) profiles at onset of instability for different Hostun RF sand specimens with varying initial void ratio e_0 (at $\sigma'_c = 400$ kPa) **a** 0.6 **b** 0.65 **c** 0.7 **d** 0.75

phase transformation occurring in the specimens when e_0 is gradually changed from 0.8 (loose) to 0.6 (dense specimen).

Figure 5 depicts the shear strain contours (ε_q) of Hostun RF sand specimens with varying e_0 at the onset of instability (ε^b_{ao}). For a dense specimen ($e_0 = 0.6$), a distinct zone of localized strain accumulation could be identified (Fig. 5a) with the shear band inclination angle (θ_s) being ~ 51°. A straight line was fit across all the points with excessive shear strain along the height of the specimen for estimating θ_s. On the other hand, in case of a medium dense sand specimen ($e_0 = 0.65$), the orientation of the shear band angle got reversed which is evident from Fig. 5b and θ_s was estimated ~ 48°. With further increase in e_0 to 0.7 and 0.75 (relatively looser specimen), θ_s was evaluated to be ~ 44.5° and 44° (Fig. 5c and d), respectively, and a single distinct zone of shearing could not be identified. In all of these cases contractive zones were found to exist adjacent to the localized dilative zone(s) indicating local fluid motion within the sand specimens although global undrained conditions were imposed on the boundaries. Interestingly, it is to be noted that with an increase in the initial void ratio (as it moves towards becoming a looser specimen), the estimated shear band angle in an undrained biaxial shearing became flatter i.e. the instability mode slowly moved towards a 'solid-fluid' type from a localized one.

5 Patch Area (A) Effect on Instability Onset for a Particular Perturbation Intensity

The effect of areal extent of material heterogeneity for a fixed perturbation magnitude on instability onset has also been examined in the present article. Coupled undrained numerical simulations for this particular case have been performed on sand specimens with 400 elements (nearly converged mesh) and $e_0 = 0.65$ at a confining pressure of 400 kPa and with an induced perturbation intensity of 1% of e_0. Spatial extent of a single element of the sand specimen under consideration has been denoted as the patch area A.

Effect of patch area (A) on instability onset has been explored by varying the number of elements in which the perturbation was introduced and this has been illustrated in Fig. 6. Undrained biaxial shearing of Hostun RF sand revealed that instability onset strain (ε^b_{ao}) lowered down from ~ 1.7% for 1A to ~ 1.5% for 9A. However, a further increase in patch area to 16A and 25A did not show any variation in ε^b_{ao}. Thus, increase in spatial extent of patch area lowered down ε^b_{ao} to some extent, however it ceased to exhibit any influence when the material heterogeneity (fixed perturbation intensity) was induced over a larger area.

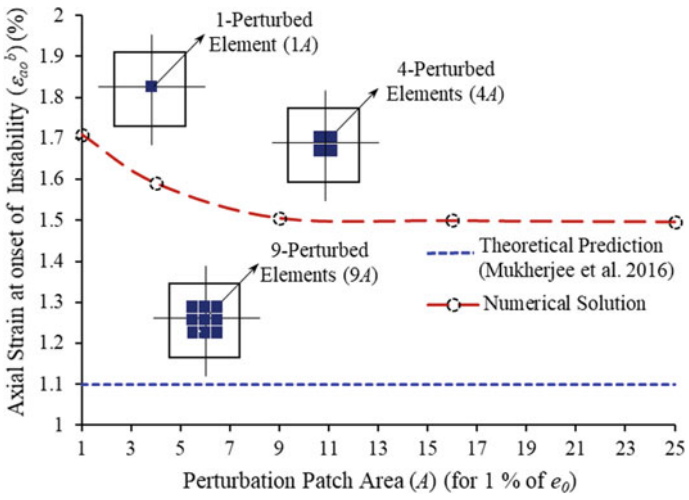

Fig. 6 Axial strain at instability onset (ε^b_{ao}) versus Patch Area (A) ($P = 1\%$ of e_0; 0.65)

6 Conclusions

Numerical investigation of instability onset in granular media has been explored in the current study by inducing material heterogeneity in Hostun RF sand specimens under biaxial loading. The F-δ response was uniform for a lesser number of elements (N = 9 or 16) even when a small perturbation (0.01% of e_0; 0.65) was introduced in the middle element. However, with mesh refinement the material behaviour deviated from its uniform F-δ response and ε_{ao}^{b} was estimated ~ 1.8% for 400 elements. Thus, instability onset in granular media (drop in F-δ) was found to be a mesh-dependent phenomenon within a numerical framework. Perturbation intensity (Pin terms of % of e_0) also had significant impact in lowering down ε_{ao}^{b} to nearly theoretically predicted value for $P = 10\%$ of e_0. Undrained biaxial shearing of Hostun RF sand specimens revealed that decrease in e_0 resulted in delayed instability onset. The emergence of localized mode of instability could be well apprehended for denser specimens ($e_0 < e_c$) whereas, initiation of strain-softening behaviour was captured for the loose specimen ($e_0 > e_c$) in which 'liquefaction-type solid-fluid' instability mode becomes the triggering mechanism. These localized dilative zones were accompanied with contractive zones adjacent to them indicating local fluid movement within the sand specimen although global undrained condition was imposed on the boundaries. Increase in spatial extent of material heterogeneity (for a fixed perturbation magnitude) leads to an early onset of instability in Hostun RF sand specimens to a certain degree and it did not exhibit any considerable effect on further increasing the areal expanse of material imperfection.

References

1. ABAQUS Inc. (2014) ABAQUS Analysis User's Manual, Version 6.14. Providence, RI, Simulia
2. Andrade JE, Borja RI (2007) Modeling deformation banding in dense and loose fluid-saturated sands. Finite Elem Anal Des 43(5):361–383
3. Aydin A (2000) Fractures, faults, and hydrocarbon entrapment, migration and flow. Mar Pet Geol 17(7):797–814
4. Bažant ZP, Jirásek M (2002) Nonlocal integral formulations of plasticity and damage: survey of progress. J Eng Mech 128(11):1119–1149
5. Bhattacharya D, Mukherjee M, Prashant A (2019) Perturbation intensity and mesh convergence in coupled undrained instability analysis in sands under biaxial loading. Int J Geomech (In Review)
6. Bésuelle P (2001) Compacting and dilating shear bands in porous rock: theoretical and experimental conditions. J Geophys Res: Solid Earth 106(B7):13435–13442
7. Borja RI, Regueiro RA (2001) Strain localization in frictional materials exhibiting displacement jumps. Comput Methods Appl Mech Eng 190(20–21):2555–2580
8. Daouadji A, Darve F, Al Gali H, Hicher PY, Laouafa F, Lignon S, Nicot F, Nova R, Pinheiro M, Prunier F, Sibille L (2011) Diffuse failure in geomaterials: Experiments, theory and modelling. Int J Numer Anal Meth Geomech 35(16):1731–1773
9. Desrues J, Georgopoulos IO (2006) An investigation of diffuse failure modes in undrained triaxial tests on loose sand. Soils Found 46(5):585–594

10. Finno RJ, Harris WW, Mooney MA, Viggiani G (1996) Strain localization and undrained steady state of sand. J Geotech Eng 122(6):462–473
11. Finno RJ, Harris WW, Mooney MA, Viggiani G (1997) Shear bands in plane strain compression of loose sand. Ge′otechnique 47(1):149–165
12. Fleck NA, Hutchinson JW (2001) A reformulation of strain gradient plasticity. J Mech Phys Solids 49(10):2245–2271
13. Gajo A, Muir Wood D (1999) A kinematic hardening constitutive model for sands: the multiaxial formulation. Int J Numer Anal Meth Geomech 23(9):925–965
14. Garagash DI (2005) Diffuse versus localized instability in compacting geomaterials under undrained conditions. In: Geomechanics: testing, modeling, and simulation, pp 444–462
15. Guo P (2013) Undrained shear band in water saturated granular media: a critical revisiting with numerical examples. Int J Numer Anal Meth Geomech 37(4):353–373
16. Guo P, Stolle DFE (2013) Coupled analysis of bifurcation and shear band in saturated soils. Soils Found 53(4):525–539
17. Han C, Drescher A (1993) Shear bands in biaxial tests on dry coarse sand. Soils Found 33(1):118–132
18. Han C, Vardoulakis IG (1991) Plane-strain compression experiments on water-saturated fine-grained sand. Ge′otechnique 41(1):49–78
19. Khoa HDV, Georgopoulos IO, Darve F, Laouafa F (2006) Diffuse failure in geomaterials: experiments and modelling. Comput Geotech 33(1):1–14
20. Lade PV, Pradel D (1990) Instability and plastic flow of soils. I: experimental observations. J Eng Mech 116(11):2532–2550
21. Mokni M, Desrues J (1999) Strain localization measurements in undrained plane-strain biaxial tests on Hostun RF sand. Mech Cohesive-Frict Mater 4(4):419–441
22. Mooney MA, Viggiani G, Finno RJ (1997) Undrained shear band deformation in granular media. J Eng Mech 123(6):577–585
23. Mukherjee M, Gupta A, Prashant A (2016) Instability analysis of sand under undrained biaxial loading with rigid and flexible boundary. Int J Geomech 17(1):04016042
24. Nicot F, Darve F (2011) Diffuse and localized failure modes: two competing mechanisms. Int J Numer Anal Meth Geomech 35(5):586–601
25. Schofield A, Wroth P (1968) Critical state soil mechanics. McGraw-Hill, London
26. Shuttle DA, Smith IM (1988) Numerical simulation of shear band formation in soils. Int J Numer Anal Methods Geomech 12(6):611–626
27. Vardoulakis I (1981) Bifurcation analysis of the plane rectilinear deformation on dry sand samples. Int J Solids Struct 17(11):1085–1101
28. Vardoulakis I (1985) Stability and bifurcation of undrained, plane rectilinear deformations on water-saturated granular soils. Int J Numer Anal Meth Geomech 9(5):399–414
29. Wood DM (2004) Geotechnical Modelling. CRC Press